Bull Volcanol (2004) 66:725–734
DOI 10.1007/s00445-004-0353-y

RESEARCH ARTICLE

John Simmons · Derek Elsworth · Barry Voight

Instability of exogenous lava lobes during intense rainfall

Received: 23 April 2003 / Accepted: 28 February 2004 / Published online: 26 May 2004

Abstract On many volcanoes, there is evidence of a relationship between dome collapse and periods of high precipitation. We propose a mechanism for this relationship and investigate the conditions that optimize failure by this process. Observations of elongate lobes that evolve through exogenous growth of lava domes reveal that they commonly develop tensile fractures perpendicular to the direction of motion. These cracks can increase in depth by localized cooling and volumetric contraction. During periods of high rainfall, water can fill these cracks, and the increase in fluid pressure on the base of the lobes and within the crack can trigger the collapse of the hot exogenous lava domes. Using limit-equilibrium analysis, it is possible to calculate the water and vapor forces acting on the rear and base of the potentially unstable part of the lobe. The model presented is rectangular in cross-section, with material properties representative of andesitic dome rocks. Vapor pressures at the base of cracks are sealed by the penetrating rainfall, which forms a saturated cap within the lobe. This leads to an increase in fluid pressurization both through the underlying gas pressure and the downslope component of the liquid water cap. Fluid pressurization increases as the penetration depth increases. This rainfall penetration depth is dependent on the thermal properties of the rocks, antecedent temperature, lobe geometry, and the intensity and duration of precipitation. Dominant parameters influencing the stability of the lobe are principally lobe thickness, duration and intensity of rainfall, and antecedent lobe temperature. Our modeling reveals that thicker lobes are intrinsically more unstable due to the amplification of downslope forces in comparison to cohesive strength. The increase in the duration and intensity of rainfall events also increases the potential for collapse, as it leads to deeper liquid penetration. Deeper penetration depths are also achieved through lower antecedent temperatures since less fluid is lost through vaporization. Thus, the potential for rain-triggered collapse increases with time from emplacement.

Keywords Instability · Exogenous lava lobes · Intense rainfall

Editorial responsibility: D. Dingwell

J. Simmons (✉) · D. Elsworth · B. Voight
College of Earth and Mineral Sciences,
Penn State University,
University Park, PA 16802, USA
e-mail: john.r.simmons@exxonmobil.com

Present address:
ExxonMobil Exploration Company,
233 Benmar, Houston, TX 11060, USA

Introduction

Growing andesitic lava domes are a potential hazard on many volcanoes. Problems arise from dome collapse: the potential generation of pyroclastic flows, the triggering of subsequent eruptive activity that may generate column-collapse pyroclastic flows, widespread ashfall, and the elevated potential for lahars. Spalling of the carapace and internal dome forces, especially for the gas-infused Peléan type domes, are important contributors to collapse (Voight 2000). Potential mechanisms for these failures include slope oversteepening by erosion and piping (Fink and Griffiths 1998; Sparks et al. 2000), generation of gas or fluid overpressurization within a weak underlying stratum (Lopez and Williams 1993; Voight and Elsworth 1997; Crowley and Zimbleman 1997; Watters et al. 2000), the propagation of thermal fractures through the brittle rind (Yamasato et al. 1998), and gas overpressurization of the inner dome itself (Voight and Elsworth 2000; Elsworth and Voight 2001).

Numerous lava dome collapses have coincided with intense rainfall during times of low effusive growth, and absent the typical solid earth triggers of increased deformation, related seismicity, and offgassing. Merapi volcano, Central Java, Indonesia, Soufrière Hills volcano, Montserrat, B.W.I., Unzen volcano, Kysushu, Japan, and Mt. St. Helens all have a history of instability correlated with intense rainfall (Voight et al. 2000; Matthews et al.

2002; Yamasato et al. 1998; Mastin 1994). The potential overpressurization of the dome by rainfall-induced fluid overpressures has also been investigated for the endogenous dome of Soufrière Hills volcano. This approach (Elsworth et al., unpublished data) has defined the effects of rainfall infiltration on the distribution, timing, and magnitude of gas overpressurization and its influence on the collapse of endogenous domes. This approach may be extended to examine rainfall-related collapses of exogenous domes. At least four dome collapse-events on the exogenous-dome-growth dominated Merapi volcano (Voight et al. 2000) and upwards of 18 collapse events on the exogenous-dome-growth dominated Unzen volcano (Yamasato et al. 1998) have been associated with heavy rainfall. In addition, it is suggested (Voight et al. 2000; Ratdomopurbo and Poupinet 2000; Yamasato et al. 1998) that rain infiltration has played a role in Merapi and Unzen dome collapse events, although no models have been developed for this type of triggering mechanism.

In this contribution, we investigate the importance of hydraulic penetration of rainfall into the fractured surface of exogenous lobes, its potential to both develop and seal-in gas overpressures, and the likely influence of these overpressures on instability. The focus is on the evolution of instability of exogenous lava lobes during periods of intense precipitation. Where powerful storms can trigger the collapse of exogenous domes, a rational model offers the potential to define the conditions that lead to collapse. These include rainfall intensity and duration and the shape and thermal state of the dome. Instability is described via a limit-equilibrium model that incorporates rainfall-induced fluid overpressures. Fluid overpressures are modulated by rainfall intensity and duration, thermal controls on water infiltration and vaporization in the hot lobe interior, the ability to contain these pressures laterally across strike, and the ability of a saturated rind to cap these pressures. Calculated fluid pressures are used to provide order of magnitude estimates of destabilizing forces and to evaluate the likelihood of collapse. The methodology also leads to the determination of the likely timing and severity of failure.

Stability model

Exogenous lobes are typically elongate fingers of viscous lava that drape the flanks of a volcano down-slope of an eruptive vent (Fig. 1a). Transport of the stiffening lava is driven by both lava effusion and gravity and is temporarily arrested by rheological-stiffening related to the loss of volatiles (Sparks et al. 2000). The resulting lobes comprise disjointed fingers resting on an inclined surface (Fig. 1b). A force-balance may be completed on the free-body isolated at the lobe toe, enabling the relative stability to be defined as a "factor of safety", F_S. The factor of safety is defined as the ratio of forces resisting failure to those promoting failure, resolved relative to the direction of potential failure. Correspondingly, the evolving instability of lava lobes during intense storm events is influenced by the amount of down-slope and uplift forces

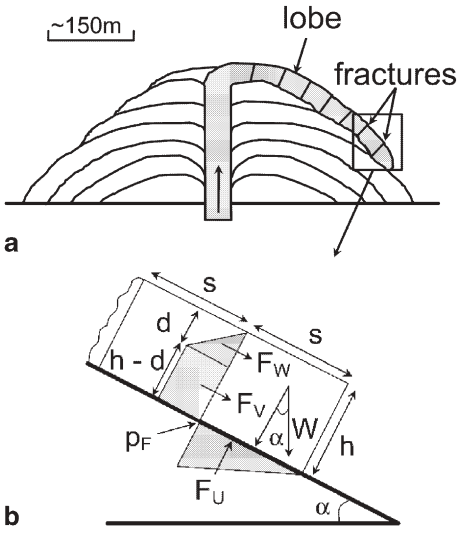

Fig. 1 Schematic view of potential forces acting on a lava lobe block due to rain infiltration. **a** Two-dimensional macro-view of generic exogenous lava lobe. **b** Section through the two bottom-most blocks of a lava lobe of height h, and fracture spacing s, which rests on the volcano flank, inclined at angle, α. The bottom-most block, having weight W, is disturbed by down-slope forces acting on the block rear, representing pressures due to rain infiltration to depth d (specifically vapor pressures F_V, and water pressures F_W), and uplift forces (F_U) acting on the block bottom, representing pressures due to the infiltrating rain water/vapor, p_F

produced by rainwater infiltration and subsequent build-up of vapor pressures, together with material rock properties and the geometry of particular lobes.

The geometry of Fig. 1b considers the lowermost portion of a lobe of thickness, h, and inclination, α, isolated by a fracture of spacing, s, that cuts the full depth of the lobe. During a storm, rainfall penetrates the fracture as liquid to a depth, d, and caps vapor pressures below, as conditioned by the controlling thermal hydrology (discussed later). The liquid pressure is hydrostatic and prescribes the upper limit of the underlying vapor overpressure as $\gamma_W\, d\cos(\alpha)$, where γ_W is the unit weight of water, defined as the product of water density, ρ_W, and gravitational acceleration, g. The limiting equilibrium for the geometry of Fig. 1b may be defined relative to the disturbing influence of the down-slope components of the water, F_W, and vapor forces, F_V, and by the vapor uplift force, F_U, applied to the basal plane. Correspondingly, the factor of safety may be defined for a unit thickness of slope as,

$$F_S = \frac{c_s + (W\cos(\alpha) - F_U)\tan(\phi)}{W\sin(\alpha) + F_W + F_V} \quad (1)$$

where c is the cohesive strength, ϕ is the friction angle, block weight $W{=}s{\times}h{\times}\gamma_R$, uplift force $F_U{=}1/2\ d\cos(\alpha){\times}\gamma_W{\times}s$, vaporized water force $F_V{=}d\cos(\alpha){\times}\gamma_W{\times}(h{-}d)$, liquid water force $F_W{=}1/2\ d^2{\times}\cos(\alpha){\times}\gamma_W$, where γ_R is the unit weight of the rock, defined from the rock density, ρ_R, as $\gamma_R{=}\rho_R\ g$, and all other components are identified in the geometry of Fig. 1. Values of $F_S{\leq}1$ imply failure.

Rainwater will infiltrate the lobe, principally along fractures, to a depth determined by both thermal controls and lobe geometry. If sufficiently chilled by this, and prior quenching, the infiltrating liquid will act as a near-impervious "cap" trapping the underlying overpressures as the liquid at the infiltration front flashes to steam. The vapor overpressure is limited by the supernatant water pressure, with a small additional contribution from the air entry pressure, ignored in this treatment. Without a "cap" to contain the vapor pressure, the uplift force and down-slope destabilizing forces arising from this vapor pressure are absent. Note also that the down-slope destabilizing forces reach a maximum when water is able to penetrate to the base of the block.

Thermal hydrology

The ability to develop a saturated cap that both traps the underlying gas pressure and provides a down-slope component of liquid pressure is controlled by the ability of fluid to penetrate the lobe. This penetration is in turn controlled by the ability of the cooling lobe to vaporize the rainfall. Multiple rainfall events will quench the lobe surface, enabling successive rainfall to penetrate more deeply. The growth of penetration with time may be estimated by considering the thermal hydrology of the lobe.

The thermal hydrology is conditioned by the rock and fluid thermal conductivities, densities, and heat capacities. Although not measured, feasible magnitudes are included in Table 1. Hydraulic penetration to depth d into a ubiquitously fractured lobe of fracture spacing s may be estimated by equating the quenching potential (thermal flux) of rainfall, discharged from a tributary catchment area into a fracture, with the thermal flux conducted across the fracture wall as the penetrating water chills the margin to below boiling. If the tributary catchment on either side of the fracture is the half spacing, l=s/2, then an energy balance may be defined for the geometry of Fig. 2a. Thermal flux of magnitude Q_T is removed from the face of the fracture as rainwater, gathered on the surrounding catchment and discharged into the fracture, is spontaneously vaporized. For a unit width of the system, w, the penetration depth, d, may be evaluated by equating the thermal flux expended in cooling the fracture surface by an amount T_R, and raising the water from ambient temperature to boiling, T_W. The minor contribution of the latent heat of vaporization is omitted. Assuming that the ground surface has been chilled, such that the full quantity of rainfall reaches the fracture, and that heat flow to the fracture is solely horizontal, the system is reduced to one dimension. The temperature drop at the face may be defined as (Carslaw and Jaeger 1959)

$$Q_T = \frac{2\lambda_R \Delta T_R}{s[t_D + f(t_D)]};$$

$$f(t_D) = \frac{1}{3} - \frac{2}{\pi^2}\sum_{n=1}^{\infty}\frac{(-1)^n}{n^2} e^{-t_D n^2 \pi^2} \cos(n\pi), \qquad (2)$$

Table 1 Summarized properties of andesitic dome rocks and associated fluids

Dome rocks			
Property	Symbol	Typical value	Units
Density[a]	ρ_R	2,600	kg/m^3
Specific heat[b]	c_R	918	J/kg°C
Thermal diffusivity[b]	K_R	1.14×10	m^2/s
Permeability[c]	k	10–10	m^2
Fluid diffusivity[a]	K_F	1.16×10–1.16×10^0 (~10^2–10^5)	m^2/s (m^2/d)
Cohesion[a]	c	0.1, 0.5	MPa
Friction angle[a]	ϕ	45, 25	°
Temperature[d]	T_R	200–800	°C
Fracture spacing[d]	s	1–100	m
Lobe thickness[d]	h	50–100	m
Slope angle[d]	α	30–35	°
Water			
Density[b]	ρ_W	1,000	kg/m^3
Specific heat[b]	c_W	4,187	J/kg°C

[a] Voight and Elsworth (2000)
[b] Elsworth (1989)
[c] Woods et al. (2002)
[d] Nakada et al. (1999)

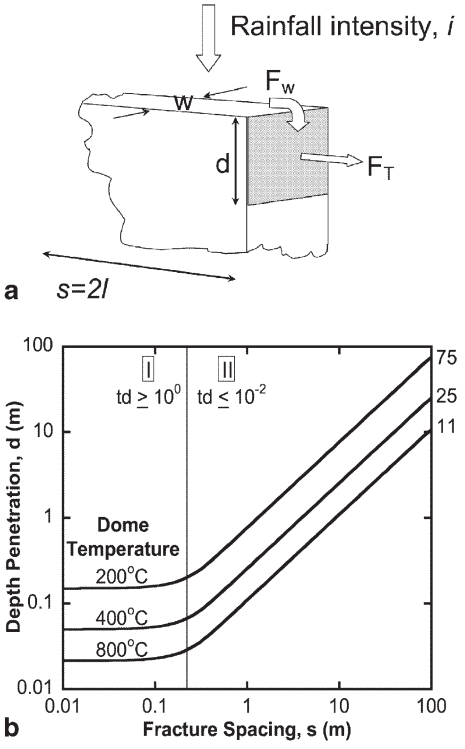

Fig. 2 Controls on quenching at the dome surface. **a** Geometry describing a simplified thermal hydrology of a quenched surface containing vertical fracture pathways. **b** Quenching depth penetration d for a discrete storm discharging 75-mm-rainfall over 3 h. *Area I* defines d for values of $t_D \geq 10^0$, which represents the case of (very) closely fractured media. *Area II* defines d for values of $t_D \leq 10^{-2}$, which represents the case of either short duration rainfall events or widely spaced fractures. Material parameters are defined in Table 1. Enumerated for fractures spaced 100 m apart, are penetration depths d of 11, 25, and 75 m, in dome lavas at initial temperatures of 800, 400, and 200 °C, respectively

where λ_R is the thermal conductivity of the rock and t_D is a diffusive time, defined both by the thermal diffusivity of the rock, K_R, and the duration of the rainfall event, t, as $t_D = K_R t / l^2$. Similarly, the thermal flux due to the quenching fluid, Q_W, may be defined as

$$Q_W = i \rho_W c_W \Delta T_W, \quad (3)$$

for rainfall of intensity, i, and water constants of density, ρ_w, and specific heat, c_W. Equating the fluxes of Eqs. (2) and (3) through their tributary areas yields $Q_W w l = Q_T w d$, and enables a nondimensional depth penetration, d, to be defined in terms of fracture spacing, $s = 2l$, as

$$4 \frac{\kappa_R d}{i s^2} = \frac{\rho_W c_W}{\rho_R c_R} \frac{\Delta T_W}{\Delta T_R} [t_D + f(t_D)]. \quad (4)$$

For anticipated lobe temperatures in the range 200–800 °C, Eq. (4) is shown in Fig. 2b for a rainfall event typical of collapse-triggering deluges at Montserrat, i.e. 75 mm in 3 h, an event not atypical of Merapi [storm intensities of 25 mm/h comprised ~5% of 1990 storms on Merapi (Lavigne et al. 2000)]. Two limiting behaviors are apparent. For (very) closely fractured media, thermal equilibrium is reached in the saturated surface concurrent with the rainfall (no horizontal thermal gradient is sustained). This is apparent for $t_D \geq 10^0$ where the summation term of Eq. (4) is null, and depth penetration is defined as

$$d = \frac{\rho_W c_W}{\rho_R c_R} \frac{\Delta T_W}{\Delta T_R} (t \times i) \cong \frac{2}{1} \frac{\Delta T_w}{\Delta T_R} (t \times i). \quad (5)$$

For quenching from 800 °C, this represents a minimal depth penetration of about one quarter of the total rainfall amount, and for quenching from 200 °C, the penetration approximates the rainfall amount. This penetration of several centimeters will be insufficient to generate significant overpressures.

The second limiting behavior is for rainfall duration of $t_D \leq 10^{-2}$, which represents either shorter duration events (relative to thermal diffusivity) or widely spaced fractures. For fracture spacing typical (5–100 m spaced fractures and faults) of lobe environments, this behavior mode prevails and is represented in Fig. 2b. Here, depth penetration increases in proportion with spacing and is approximated as

$$d \cong \frac{i s^2}{4 \kappa_R} \frac{\rho_W c_W}{\rho_R c_R} \frac{\Delta T_W}{\Delta T_R} [1.13 \sqrt{t_D}]. \quad (6)$$

This relationship represents the case where the rainfall event chills the fracture margin but does not significantly cool the interior. This is the behavior of interest in promoting collapse that develops concurrently with the rainfall event. If the collapse is significantly delayed, remnant heat will slowly remove the penetrating water.

As can be seen in Fig. 2b, possible depth penetrations are of the order of 0.5–11 m for the hottest case of an 800 °C lobe for fracture separations of 5–100 m. If the lobe has been cooled by multiple prior events, depth penetration to 25 m is feasible at average lobe temperatures of 400 °C and 75 m at 200 °C, each for the most widely spaced fractures (100 m). Importantly, the quenching of the hot lobe surface will result in the downward propagation of surface-normal cracks (Nemat-Nasser et al. 1978). As the cracks deepen and lengthen, their tip zones will interact and every-other fracture will grow at the expense of the intervening fracture, which will remain dormant and static. This process may repeat itself resulting in fractures spaced at either two, four, or eight times the initial spacing, depending on the temperature profile and depth of the system. In other words, the positive feedback of the most open seed fracture, which accepts quenching fluid that chills its margins and enlarges and deepens it, allows it to preferentially accept more water from subsequent storms.

Parametric analysis

By combining the description of the limit-equilibrium behavior of the lobe with the anticipated influence of infiltrating rainwater, the evolution of instability within the slope may be followed. A parametric evaluation is completed to define the relative influence of the variety of interacting processes on the resulting behavior, and to define critical processes. A standard configuration, representative of lobe geometries at Merapi and Unzen, is selected with block heights in the range 50–100 m, and slope inclination of 34° (Table 1, estimated from Figs. 3, 31, and 32 of Voight et al. 2000; documented explicitly in Nakada et al. 1999). Typical values for cohesion and friction pairs for andesitic lavas (0.5 MPa and 25°; 0.1 MPa and 45°) are also selected, representative of rock mass strengths for hot lavas at Soufrière Hills volcano (Voight and Elsworth 2000; Elsworth and Voight 2001; Voight et al. 2002). The baseline storm threshold is an event with intensity of 25 mm/h lasting for 3 h, as representative of thunderstorm activity in the tropics, in general, and at Merapi and Soufrière Hills volcanoes, in particular (Lavigne et al. 2000; Matthews et al. 2002).

Trends in behavior

Instability is conditioned by lobe geometry and antecedent temperature, the strength of materials comprising the lobe, and by the intensity and duration of rainfall. By systematically varying the parameters controlling instability, the relative contribution of various processes may be isolated. Critical variables considered in this manner are block height, h, fracture spacing, s, lobe temperature, T_R, slope angle, α, rainfall intensity and duration, cohesion, c, and friction angle, ϕ. In many cases a mean lobe temperature of 400 °C is conservatively used when temperature is held constant, relative to other parameters, where the roles of related processes are desired.

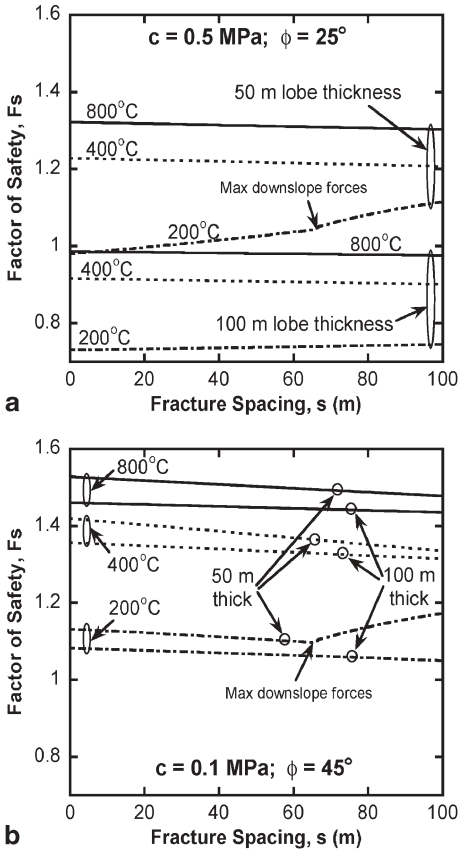

Fig. 3 Variation in factor of safety of a lava lobe exposed to a rainfall event totaling 75 mm in 3 h due to different lobe temperatures, geometries, and rock strengths. For the 50-m-thick lobe with initial temperature of 200 °C, maximum down-slope forces are attained when $s \geq 67$ m because liquid water reaches the bottom of the fracture. **a** Strength: c=0.5 MPa and ϕ=25°; slope angle is 34°. The 100-m-thick lobe is unstable regardless of fracture spacing and temperature. **b** Strength: c=0.1 MPa and ϕ=45°; slope angle is 34°

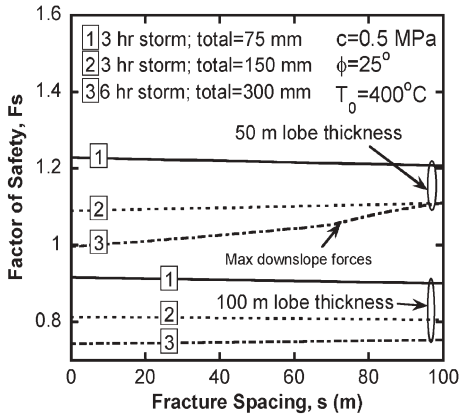

Fig. 4 Variation in factor of safety due to different rainfall intensities and durations. Initial temperature of the lobe is 400 °C; strength: c=0.5 MPa, ϕ=25°; slope angle is 34°

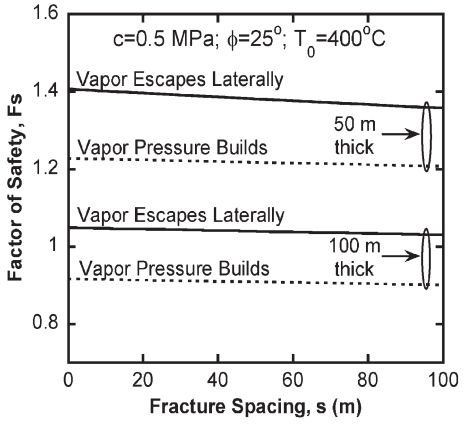

Fig. 5 Variation in factor of safety between the case of zero water vapor forces acting (due to high lateral permeability allowing gases to escape), and the case in which water vapor forces are allowed to build. Initial temperature of the lobe is 400 °C; strength: c=0.5 MPa, ϕ=25°; slope angle is 34°

Lobe geometry

The variation of factor of safety with fracture spacing, for lobe thicknesses of 50 and 100 m, is shown in Fig. 3. Lobe geometry has a significant influence on instability. Instability is controlled principally through the absolute magnitude of lobe thickness, or corresponding block height, with a more modest influence of toe-block length, represented through fracture spacing, s. Thinner lobes exhibit higher relative stability due to the dominance of cohesive resistance at the low stress levels apparent for the thinner lobe. In general, lobe thicknesses of 100 m return a factor of safety ~0.3 lower than those representing a height of 50 m (Fig. 3a, Figs. 4, 5, and 6). This effect dominates the influence of other parameters making block height arguably the most important parameter in defining stability.

In most cases, factor of safety decreases slightly with increased fracture spacing because the tributary catchment area for each fracture increases with greater spacing between fractures. A larger tributary area results in a greater availability of water for each fracture during any given storm. However, for a static average lobe temperature, fracture spacing has a relatively minor effect on stability, and this is most apparent where cohesion dominates the response (Fig. 3a). For a rainfall event of 25 mm/h lasting 3 h and a lobe at 400 °C (regardless of cohesion and friction values), fracture spacing of 100 m has a factor of safety only ~0.01–0.02 lower than that of 50 m (Fig. 3b). This apparent minor influence of rainfall on instability both ignores the role of deluge in lowering the lobe temperature over the long-term, through exposure to multiple events, and the critical influence that a small drop in factor of safety may play in ultimately triggering the collapse of a lobe brought progressively closer to failure. Depending on the amount of rain, and the choice of temperature, and cohesive and frictional strengths, factor of safety can both increase and decrease with fracture spacing. Such increases in stability can be attributed to the dominance of cohesion at low tempera-

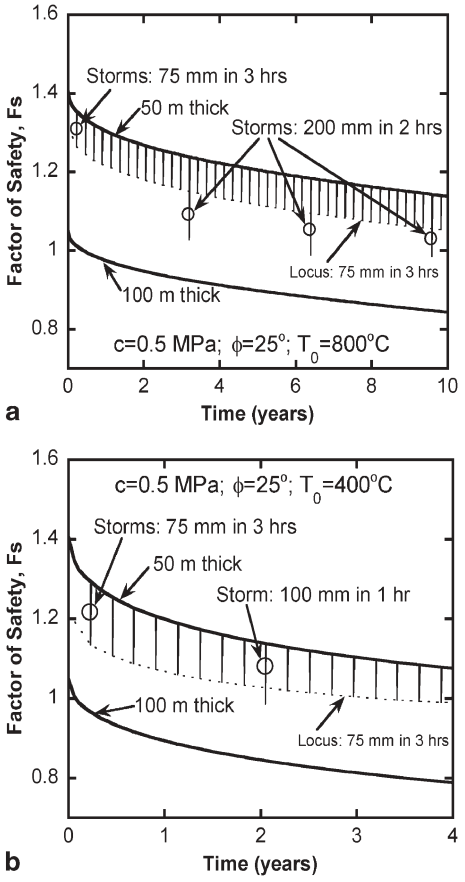

Fig. 6 Variation in factor of safety over time; pertinent parameters: c=0.5 MPa, ϕ=25°, α=34 °, s=50 m. *50 m-thick lobe* upper bound defines factor of safety for a constant rainfall event equal to the high average annual rainfall at Merapi (4.5 m), lower bound defines factor of safety locus due to isolated storm events of 75 mm over a 3-h period. *100 m-thick lobe* factor of safety defined for a constant rainfall event equal to the high average annual rainfall at Merapi (4.5 m) only. Marginal stability decreases to $F_S \leq 1$ in a matter of months. **a** Variation for period of time from emplacement (initial temperature=800 °C) to possible failure. Marginal stability for a 50-m-thick lobe decreases to $F_S \leq 1$ for well-timed storm totaling 200 mm in 2 h. **b** Variation for period of time from an initial lobe temperature of 400 °C to possible failure. Marginal stability for a 50-m-thick lobe decreases to $F_S \leq 1$ for well-timed storm totaling 100 mm in 1 h or 75 mm in 3 h

tures and during extreme deluge, i.e. greater basal contact area results in greater stability (Figs. 3a and 4).

Slope angle must be considered as an important factor in lobe stability because small changes in slope angle can make marked changes in factor of safety. For the conservatively chosen 400 °C dome with 100-m-block height, 50-m-spacing, and 25 mm/h lasting 3 h-rainfall event, factor of safety increases by ~0.26 between a 40° slope and a 30° slope. Locally, however, the slope angle beneath a particular lava lobe is not subject to as much variation as lobe thickness. Since slope angle is generally well constrained, large variations are not necessary to consider for a particular site.

Temperature

In the regime where fractures act as a dominant agent in advecting percolating rainwater into the lobe interior, rainfall penetration depth at any given mean lobe temperature is linearly related to fracture spacing (Fig. 2b). Correspondingly, the factor of safety is calculated for lobes at mean temperatures of 200, 400, and 800 °C, subject to a rainfall event of 25 mm/h lasting for 3 h. This corresponds to penetration depths of: $d \approx 0.75 \times s$ (at 200 °C); $d \approx 0.25 \times s$ (at 400 °C); and, $d \approx 0.11 \times s$ (at 800 °C).

Not surprisingly, high temperatures result in overall greater stability than low temperatures (Fig. 3), due to the inability of the water to significantly penetrate the hot lobe and elevate pressures. A rainfall event of 25 mm/h lasting 3 h, on a 100-m-thick lobe at a temperature of 200 °C (50 m spacing), yields a factor of safety ~0.16–0.27 lower than a dome at 400 °C (depending on cohesion and friction values used). A dome at 800 °C has a factor of safety of only ~0.07–0.11 higher than a dome at 400 °C for the same block dimensions and rainfall event (depending on cohesion and friction values used). The reason that doubling temperature from 200 to 400 °C has a greater effect on F_S than doubling temperature from 400 to 800 °C is that the depth that water can penetrate at 200 °C ($d \approx 0.75 \times s$) is 3 times greater than at 400 °C ($d \approx 0.25 \times s$), while the depth that water can penetrate at 400 °C is only 2.3 times greater than at 800 °C ($d \approx 0.11 \times s$)—the downslope destabilizing force is proportional to the square of the penetration depth.

Rainfall intensity and duration

As would be expected, doubling rainfall intensity and keeping the duration of the rainfall event the same approximately doubles the rainfall penetration (e.g. $d \approx 0.25 \times s$ at 400 °C for 25 mm/h and 3 h, $d \approx 0.5 \times s$ at 400 °C for 50 mm/h and 3 h). For a 100-m-thick lobe at 400 °C with a fracture spacing of 50 m, the factor of safety decreases by ~0.1 when intensity is doubled from 25 mm/h for 3 h to 50 mm/h for 3 h (Fig. 4). If both intensity and duration are doubled to 50 mm/h for 6 h, the factor of safety decreases by ~0.15 for the same conditions (Fig. 4). Thus, rainfall intensity and duration play a significant role in potentially triggering the destabilization of exogenous domes. Since rainfall penetration depth is strongly conditioned by both the deluge volume (product of intensity and duration) and lobe temperature, these three parameters are importantly linked in defining the potential for instability, as can be seen in Eqs. (4) and (6) and Fig. 2b.

When, for a given threshold fracture spacing, rainfall penetration reaches the bottom of the fracture (i.e. high rainfall intensity and duration along with low temperature), the down-slope forces are at their maximum value. Lobes containing more widely spaced fractures are restricted to this threshold pressure, and cannot develop

down-slope forces in excess of this magnitude. In this instance the factor of safety distinctively increases with an increase in fracture spacing (Fig. 3a, b) as the restoring force applied by the increasing basal length correspondingly increases. This occurs for both cohesion (Fig. 3a) and friction (Fig. 3b) dominated systems, and occurs at lesser fracture spacing as the magnitude of the deluge increases (Fig. 4). Conversely, where the infiltrating water is unable to reach the fracture base, down-slope forces always increase with an increase in fracture spacing, and the derivative of factor of safety with respect to fracture spacing never achieves a distinct increase.

Combined mechanical (strength) and geometric effects

Mechanical and geometric effects exert important controls on instability. Where cohesion dominates over frictional resistance (Fig. 3a), water pressures serve only to provide a down-slope destabilizing component, strength is little affected, and the impact of the down-slope force diminishes as block length increases. Correspondingly (Fig. 3a), factor of safety changes little with an increase in block length, but is strongly affected by lobe thickness. For an angle of sliding friction significantly less than 25°, the factor of safety would actually increase with increased fracture spacing, as the role of cohesion dominates. Conversely, where frictional behavior dominates, the impact of fluid pressures on instability is enhanced, and the drop in factor of safety with increased spacing (and water penetration) is greater (see Fig. 3b relative to Fig. 3a) than the cohesion-dominant case. Where friction dominates, lobe thickness exerts little impact on the relative degree of instability.

Lateral dissipation of gas overpressures

The potential for gas overpressures to escape, either from the lobe periphery, or via hydraulic short-circuiting within lobe interior, must also be considered. The controlling factor for each of these mechanisms relates to the lateral extent of the lobe, across strike, relative to the lobe height. Typical lobe geometries are of the order of 50–100 m thick (Voight et al. 2000, estimated from Figs. 3, 31, 32; Nakada et al. 1999, explicitly documented), and of the order of 200–300 m wide (Voight et al. 2000, estimated from Fig. 33; Nakada et al. 1999, explicitly documented).

Where lobe-width is of the order of lobe-height, the cooling of the periphery will contribute significantly to the increased penetration depth of rainfall and partially offset the increase in stability that results when the water "cap" cannot prevent lateral gas migration. Where this lateral seal is absent, fluid pressures acting on the rear scarp and on the basal detachment plane (unless liquid water reaches the bottom of the fracture) will be largely absent. Water pressures will still fully develop, as allowed by the thermal hydrology, and instability may be adequately evaluated by merely setting $F_V=F_U=0$.

At 400 °C, a 100-m-thick lobe with 50-m-fracture spacing fails when water vapor pressure is allowed to build (for a rainfall event of 25 mm/h lasting 3 h), but the block is stable when water vapor pressure escapes laterally (Fig. 5). The absence of gas overpressures is assumed unlikely given the geometry of the lobe and the likelihood of enhanced chilling, and therefore increased fluid penetration, in the lobe periphery.

Collapse potential

All effects of the various parameters examined are compounded by changes in block height. Estimates of the cohesive and frictional strength of andesitic dome rocks are available from field observations of spines (Voight 2000; Elsworth and Voight 2001), and possible strengths come in cohesion and friction pairs of drastically different values. Sliding friction properties of andesite debris show a more limited range (Voight et al. 2002), but apparent cohesions can be developed from roughness of the sliding surface. Lobe thicknesses may also vary considerably from one site or eruptive event to another. Barring extremely different values of cohesion and friction, the most important factors influencing the instability of exogenous lobes during powerful deluges, in ranked order of importance, are lobe thickness, deluge volume (product of intensity and duration), and antecedent lobe temperature. These final two environmental factors control the active triggering of instability.

During March to June 1993, the dacitic dome of Unzen volcano experienced numerous collapses resulting in pyroclastic flows during periods of rainfall (Yamasato et al. 1998). The lobe that these collapses originated from, lobe number 11, was the largest in Unzen's history, making it over 100 m thick, over 300 m wide, and over 400 m long (Nakada et al. 1999). Yamasato et al. (1998) suggest extensive fracturing due to quenching by rainfall was responsible for the collapses. However, given the model developed here, the large geometry is likely to have been the key factor, allowing for sufficient down-slope forces to build and subsequently trigger these collapses. The fact that this lobe was rather young during these failures (Yamasato et al. 1998), and therefore hot, does not detract from the feasibility of the rainfall-induced overpressurization mechanism because of its massive size, especially thickness.

The prior calculations confirm the feasibility of rainfall-induced collapse of exogenous lava domes. Several different combinations of geometry, temperature, and rainfall event are considered "favorable" conditions for failure. Factor of safety steadily decreases as dome temperature is decreased and as the amount of rain is increased, inferring that severe weather can have a profound effect on the stability of exogenous lava domes. Although better constraints are needed for this model to be applied

in specific risk assessments, the possibility of collapse causation by intense precipitation is supported.

Importantly, the process of rainfall-triggered collapse must be put into an appropriate context. While it is suspect that a single storm event could induce a catastrophic collapse of a previously stable lava dome, in the absence of other contributing factors (i.e. internally produced gas overpressures, seismic activity, etc.), it is feasible that an aging lobe that has been significantly cooled by both exposure to the atmosphere and successive storms and also weakened by extensive movement down-slope, could fail as a result of intense storm activity. Of course, one remaining question may be how intense, and for what duration, must this storm prevail. We address this in the following.

Expected failure sequence

Observed failures at Merapi (12 October 1920, 18 December 1930, 27–28 November 1961, and 10 October 1986), Unzen (at least 18 events from June 1991 to September 1993), and Soufrière Hills (3 July 1998, 20 March 2000, and 29 July 2001) have required a cumulative exposure to successive storms or an encounter with a storm of a threshold intensity and duration before a collapse occurs (Voight et al. 2000; Elsworth et al., unpublished data). The reduction in stability with time may result from either a change in the strength of lobe materials subject to multiple quenching events, or an amplification of induced fluid pressures, as water penetrates successively deeper into the lobe. These mechanisms act additively, although the strength reduction resulting from the decrease in effective stresses is expected to dominate at the short timescale of interest here. Additionally, the zone of reduced effective stresses (and strength) pervades the entire unstable lobe, and is not restricted to the zone of active fluid penetration—the influence is much more widespread. Consequently, the monotonic growth in depth-penetration of the influent rainfall, with time, may be used to define the cumulative effect of rainfall in advancing the lobe to ultimate collapse.

To forecast when a particular lobe will detach, and the corresponding storm event necessary to induce this failure, the increase in depth to which water can infiltrate over time due to cooling of the lava lobe must be ascertained. This progressive cooling of the lobe results from both quenching by rainfall and by exposure to air at ambient temperatures. The relative importance of these effects in reducing the effective lobe temperature may be estimated by a variety of conceptualizations. The change in mean lobe temperature over periods of years to decades may be estimated for the effects of (1) quenching by cumulative rainfall and (2) conductive cooling to an ambient air temperature at the lobe surface. The stability decrease, with respect to the same time scale, may be approximated from the consideration of the localized effects of cumulative rainfall in fractures "spiked" by brief superposed deluges. These effects are examined in the following.

Climatic rainfall-quenching

The average rate of cooling due to rain falling across the entire lobe surface, rather than being distributed primarily in isolated fractures, may be estimated by equating the quenching potential of the rain to the thermal energy stored in the upper portions of the penetrated lobe. Assuming a single storm event drops rainfall to a height, $t\times i$, on the lobe, and that it falls on a lobe of thickness, h, the resulting steady change in rock temperature, ΔT_R, may be straightforwardly determined as

$$\Delta T_R = \frac{\Delta T_W \rho_W c_W (t \times i)}{\rho_R c_R h}, \tag{7}$$

where ΔT_W is the change in temperature of water from ambient temperature to boiling. A 50-m-thick lobe is cooled by ~13 °C per year by rain alone if the highest average annual rainfall for Merapi, 4.5 m (Lavigne et al. 2000), is assumed.

Climatic air-cooling

Additively to the quenching effect of the rainfall, the application of ambient air temperature will also cool the surface. The time required for the lobe to cool by thermal diffusion is characterized by the dimensionless time, t_D (Carslaw and Jaeger 1959):

$$t_D = \frac{\kappa_R t_{extr}}{h^2}, \tag{8}$$

where t_{extr} is the elapsed time following extrusion, and h is the thickness of the lobe resting on an insulating boundary. Cooling to 50% with respect to ambient air temperature, of an initial lobe temperature of 800 °C, corresponds to t_D~0.2. From this it is apparent that a 50-m-thick lobe in an otherwise dry environment will air-cool at ~28 °C per year. To a reasonable approximation, the rates of rainfall-quenching and air-cooling may be considered additive, resulting in a combined rate of ~41 °C per year. These suggest that chilling of the lobe from 800 °C to mean temperatures in the range 200–400 °C, used previously, is feasibly on the timescale of years to a decade. This provides the context to view the superposed influence of major deluges, as triggers for collapse, evaluated in the following.

Climatic effects and superposed deluge triggers

Of greatest influence in the investigation of instability is the wall-temperature of the fractures. Fracture temperature controls the depth penetration of any deluge, and the resulting evolution of the destabilizing pressure. The localized cooling effect of rainfall on fracture walls, applied

continuously over the timescale of months to decades, will monotonically reduce lobe temperatures. The effects of infrequent deluges will supplant this evolving background temperature and result in brief periods of reduced stability, possibly resulting in collapse. This overall effect may be represented by including the influence of infrequent deluges on the natural decline of the lobe temperature over time.

The approach presented in the section entitled "Thermal hydrology" is superposed on the evolving mean fracture wall temperature to define how close the lobe may be brought to incipient failure. A peak annual rainfall rate of 4.5 m/year (Lavigne et al. 2000) is applied to the lobe surface as a continuous rainfall event, and an initial lobe temperature of 800 °C is assumed. The localized fracture wall temperature at the onset of these infrequent storms is calculated in a similar manner as described in Eq. (7) with the following change:

$$\Delta T_{\mathrm{F}} = \frac{\Delta T_{\mathrm{W}} \rho_{\mathrm{W}} c_{\mathrm{W}} (t_{\mathrm{f}} \times i)}{\rho_{\mathrm{R}} c_{\mathrm{R}} d_{\mathrm{t}}}, \tag{9}$$

where d_{t} is the depth in the fracture to which the average annual rainfall has reached at time t_{f}, and ΔT_{F} is the average temperature change along fractures walls induced by the infiltrating rainwater. This approach results in an average fracture wall temperature decrease of ~39 °C/year over the course of a decade, a significantly greater decrease than 13 °C/year found previously for average annual rainfall-induced lobe temperature change. This apparent discrepancy represents the different modes of quenching. The first uniformly quenches the full lobe, and the second localizes quenching at the fracture, leaving the interior block temperature little changed.

At Merapi, there have been at least seven occurrences of 100 mm/h storm events in a 20-year period (once every ~3 years), and smaller storm events of greater than 25 mm/h occur more frequently, comprising ~5% of all 1990 storms (Lavigne et al. 2000). The destabilizing influence of these infrequent storms is superimposed on the steady rainfall boundary condition. Selected, are infrequent storms of 75 mm in 3 h and 200 mm in 2 h, at respective frequencies of 4/year and 0.3/year. Cumulatively, these discrete events account for less than 10% of the distributed rainfall. Calculations are made with the cohesion and friction values that render the lowest factor of safety: hence c=0.5 MPa and ϕ=25°. The evolving factor of safety is evaluated by combining these two effects, as illustrated in Fig. 6a. The analysis omits the influence of atmospheric cooling, which would advance the lobe closer to failure at all times considered.

Figure 6a illustrates the deterioration to collapse of a 50-m-thick lobe, fractured at 50-m-intervals over a decade. The lower locus of stability for the 50-m-thick lobe is defined by the decrease in factor of safety caused by storm events. As evident in Fig. 6a, the average annual rainfall alone cannot induce failure in the 50-m-thick lobe over the decade considered, nor can 75 mm of rain in 3-h-storm events. However, if a well-timed storm of 100 mm/h, lasting 2 h, occurs after about 6 years following lobe-emplacement, failure is likely. A storm of this same duration and intensity brings the lobe very close to failure at ~3.2 years. Also noteworthy from Fig. 6a is that the average annual rainfall alone, not considering acute storm events, can bring a 100-m-thick lobe to failure in less than 1 year following emplacement. This results from the inherent lower stability of thicker lobes, discussed previously.

As would be expected, a lobe that has already cooled to 400 °C has a much shorter time to possible failure than a hotter lobe. Figure 6b shows results for the same type of events as Fig. 6a, but with a reduced initial lobe temperature of 400 °C. In this case a storm of 100 mm/h lasting only one hour can trigger failure at greater than ~2 years. Moreover a 3-h-storm totaling 75 mm can lead to failure at greater than ~3.2 years. Again, the average annual rainfall alone can bring the 100-m-thick lobe to failure in a very short time, ca. 1.5 mo.

Conclusions

The model developed in this paper, although not linked to any one case, has shown that the stability of exogenous lava lobes during periods of intense precipitation depends principally on lobe thickness, antecedent temperature, and deluge amount. Models developed to define the influence of water infiltration, and the resulting development of interior water and gas overpressures, indicate that these effects can be sufficiently large to trigger the collapse of exogenous lobes. Evidence supporting the presumption that steam is contained within fractures, seemingly a prerequisite for failure, is provided by the fact that lobes are typically two to three times wide as they are thick, therefore allowing vapor overpressures to build along the rear scarp without excessive lateral discharge. For reasonable selections of strength characteristics, thicker lobes are intrinsically less stable, due to their inherent amplification of down-slope driving forces in overcoming cohesive resistance. Similarly, cooler lobes, corresponding to lobes of earlier extrusion, inherently allow deeper penetration of infiltrating fluids, with less loss to vaporization, and are similarly inherently closer to metastability.

These evaluations corroborate observations made at Merapi and Unzen volcanoes in which intense rain has correlated with lobe detachments. Importantly, the proposed mechanisms result in a monotonic decrease in stability with time, rendering a lobe that was initially stable, metastable. The absolute timing of failure is difficult to predict given that lava lobes are components of a dynamic geologic system, which is sensitive to many environmental influences, both internal and external. However, the monotonic advance to instability that may occur gradually, for multiple small storms or suddenly with a much larger deluge event, agrees with observations at Montserrat, Merapi, and Unzen. In either case, failure

may occur in the absence of solid earth precursory events often associated with dome or lobe collapse.

As thicker lobes are inherently less stable than thin lobes, likewise, they present an elevated hazard in mobilizing a larger volume with failure, and with the potential for increased run out. A 100-m-thick lobe detachment carries twice the destructive power of that of a 50-m-thick lobe, and because of the identification of the intrinsic instability of thicker lobes, the findings of this work are important for risk analysis. It is apparent that climatic and meteorological processes are intimately coupled with the solid earth processes responsible for volcanic activity; thus attentive meteorological monitoring and forecasting ought to be utilized in conjunction with classical solid earth monitoring in the realm of volcanic risk assessment, especially for those volcanoes situated in the tropics.

Acknowledgements This work is a result of partial support by the U.S. National Science Foundation under grant CMS-9908590. This support is gratefully acknowledged. Thoughtful review comments by Harry Pinkerton and Peter Sammonds are appreciated.

References

Carslaw H, Jaeger J (1959) Conduction of heat in solids. Oxford University Press, pp 510

Crowley J, Zimbelman D (1997) Mapping hydrothermally altered rocks on Mount Ranier, Washington, with airborne visible/infrared imaging spectrometer (AVIRIS) data. Geology 25:559–562

Elsworth D (1989) Thermal permeability enhancement of blocky rocks: plane and radial flow. Int J R Mech Min Sci 26(3/4): 329–339

Elsworth D, Voight B (2001) The mechanics of harmonic gas pressurization and failure of lava domes. Geophy J Int 145:187–198

Fink J, Griffiths R (1998) Morphology, eruption rates, and rheology of lava domes: insights from laboratory models. J Geophys Res 103(B1):527–545

Lavigne F, Thouret J, Voight B, Suwa H, Sumaryono A (2000) Lahars at Merapi volcano, Central Java: an overview. J Volcanol Geotherm Res 100:423–456

Lopez D, Williams S (1993) Catastrophic volcanic collapse: relation to hydrothermal processes. Science 260:1794–1796

Mastin L (1994) Explosive tephra emissions at Mount St. Helens, 1989–1991: the violent escape of magmatic gas following storms. Bull Geol Soc Am 106:175–185

Matthews A, Barclay J, Carn S, Thompson G, Alexander J, Herd R, Williams C (2002) Rainfall-induced volcanic activity on Montserrat. Geophys Res Lett 29(13):1–4

Nakada S, Shimizu H, Ohta K (1999) Overview of the 1990–1995 eruption of Unzen Volcano. J Volcanol Geotherm Res 89:1–22

Nemat-Nasser S, Keer L, Parihar K (1978) Unstable growth of thermally induced interacting cracks in brittle solids. Int J Solids Struct 14:409–430

Ratdomopurbo A, Poupinet G (2000) An overview of the seismicity of Merapi volcano (Java, Indonesia), 1983–1994. J Volcanol Geotherm Res 100:193–214

Sparks R, Murphy M, Lejeune A, Watts R, Barclay J, Young S (2000) Control on the emplacement of the andesite lava dome of the Sourfrière Hills volcano, Montserrat by degassing-induced crystallization. Terra Nova 12:14–20

Voight B (2000) Structural stability of andesite volcanoes and lava domes. Philos Trans R Soc Lond 358(1770):1663–1693

Voight B, Elsworth D (1997) Failure of volcano slopes. Geotechnique 47(1):1–31

Voight B, Elsworth D (2000) Instability and collapse of hazardous gas-pressurized lava domes. Geophys Res Lett 27(1):1–4

Voight B, Constantine E, Siswowidjoyo S, Torley R (2000) Historical eruptions of Merapi Volcano, Central Java, Indonesia, 1768–1998. J Volcanol Geotherm Res 100:69–138

Voight B, Komorowski J, Norton G, Belousov A, Belousova M, Boudon G, Francis P, Franz W, Heinrich P, Sparks R, Young S (2002) The 26 December (Boxing Day) 1997 sector collapse and debris avalanche at Soufriere Hills volcano, Montserrat. In: Druitt T, Kokelaar B (eds) The eruption of Soufriere Hills volcano, Montserrat, from 1995 to 1999. Geol Soc Lond Mem 21:363–407

Watters R, Zimbelman D, Bowman S, Crowley J (2000) Rock mass strength assessment and significance to edifice stability, Mount Ranier and Mount Hood, Cascade Range volcanoes. Pure Appl Geophys 157:957–976

Woods A, Sparks R, Ritchie L, Batey J, Gladstone C, Bursik M (2002) The explosive decompression of a pressurized volcanic dome; the 26 December 1997 collapse and explosion of Soufriere Hills volcano, Montserrat. In: Druitt T, Kokelaar B (eds) The eruption of Soufriere Hills volcano, Montserrat, from 1995 to 1999. Geol Soc Lond Mem 21:457–465

Yamasato H, Kitagawa S, Komiya M (1998) Effect of rainfall on dacitic lava dome collapse at Unzen volcano, Japan. Met Geophys 48(3):73–78